Reprinted from JOURNAL OF ATMOSPHERIC AND OCEANIC TECHNOLOGY, Vol. 4, No. 3, September 1987
American Meteorological Society

The Effect of Calibration of the Forward-Scattering Spectrometer Probe on the Sizing of Cloud Droplets

A. A. TSONIS

W. R. LEAITCH AND M. D. COUTURE

The Effect of Calibration of the Forward-Scattering Spectrometer Probe on the Sizing of Cloud Droplets

A. A. TSONIS

Department of Geological and Geophysical Sciences, The University of Wisconsin-Milwaukee, Milwaukee, WI 53201

W. R. LEAITCH AND M. D. COUTURE

Atmospheric Environment Service, 4905 Dufferin Street, Downsview, Ontario, Canada M3H 5T4

9 May 1986 and 10 December 1986

ABSTRACT

Cloud droplets were measured from an aircraft with an FSSP in summer cloud and in winter cloud. For 70 cloud penetrations, three cloud droplet volume spectra were derived using three different calibration schemes. The spectra were parameterized by the mean volume diameter, the effective diameter, the effective dispersion, the skewness and the kurtosis. These parameters were statistically intercompared using the Mann-Whitney test. The results show that, for the clouds studied, the mean volume diameter and the effective diameter are not significantly affected by the choice of the calibration scheme. However, the dispersion of the volume distribution, the skewness and the kurtosis are quite sensitive to the details of the calibration scheme and possibly to oscillations in the intensity of the scattered light signal, as described by Mie theory.

1. Introduction

Considerable effort has been devoted to the calibration of Particle Measuring Systems' forward-scattering spectrometer probe (FSSP) for the accurate sizing of cloud droplets. An excellent discussion of this topic is given in Dye and Baumgardner (1984). In particular, Dye and Baumgardner have illustrated some of the consequences of Mie scattering on the sizing of water droplets for a particular FSSP, as defined by the solid scattering angle to the receiver. The Mie scattering intensity response, as a function of droplet radius, has been calculated for the solid scattering angle appropriate to the FSSP pertinent to subsequent discussion (the particular probe used for the measurements to be presented herein was also discussed in Dye and Baumgardner as probe 2) and is shown in Fig. 1. On the average, an oscillation is present in the Mie response function approximately every half-micron interval and plateau regions are visible around 10 and 20 μm. Because of these features, ambiguitities result in the definition of the droplet size for almost any given intensity and can extend over several micrometers. These are especially pronounced in the 5–13 μm interval. Although Dye and Baumgardner reduce the effect of such ambiguities through redefinition of the sizing intervals, superposition of their limits on the response function in Fig. 1 clearly indicates that uncertainties cannot be eliminated. Even if limits could be defined to overcome this problem, it is unlikely that the probe-optical and electronic functions could be maintained such that it was eliminated.

It is important to understand what the consequences of the sizing calibration on cloud droplet measurements can be. Towards this end, measurements of cloud droplets made with an FSSP are examined. Different sizing calibrations are applied to the measurements and the resulting cloud droplet volume distributions are compared statistically.

2. Observations and approach

The cloud droplets were sampled in cumuliform and stratiform cloud during the summer of 1982 and the winter of early 1984. The measurements were conducted from a National Aeronautical Establishment Twin Otter aircraft over regions of central Ontario, Canada. A total of 70 cloud penetrations have been examined, 35 from each period. Cumulus cloud was most frequently observed during the summer. Because the depths and liquid water contents (LWC) of these clouds were generally greater than those of the stratiform cloud, which was more frequent during the winter, the observed droplet diameters were, on average, larger for the 1982 studies than for the 1984 studies. Therefore, the data from the two periods have been considered separately in order to elucidate some differences between calibrations which may depend upon the size of the droplets.

The FSSP was maintained on size range 3, which determines the electronic gain applied to the scattered signal and which is the size range discussed by Dye and Baumgardner.

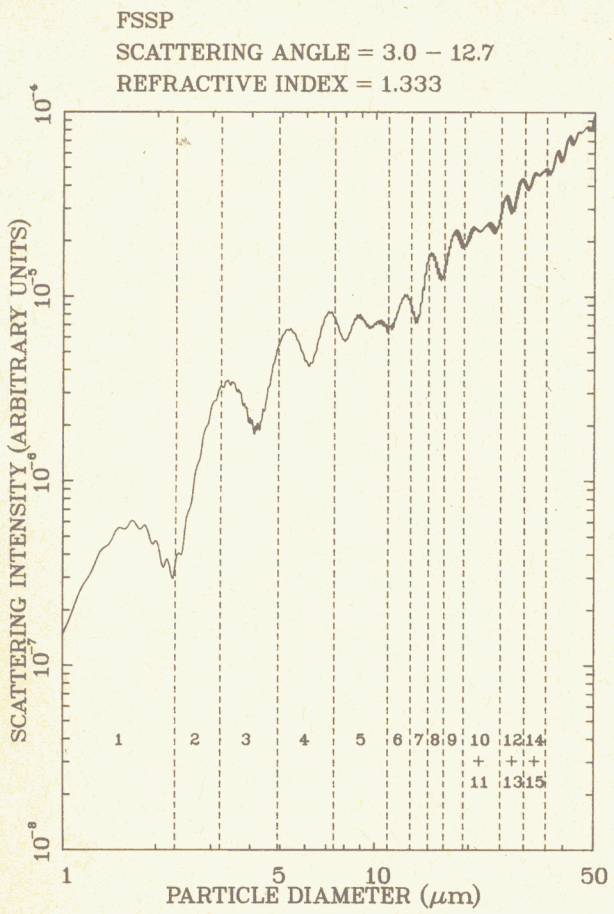

FIG. 1. The scattering response function, according to Mie theory, for the FSSP used in this study. The curve is for an index of refraction of 1.33 and the ordinate units are same as to those of Dye and Baumgardner (1984). Their sizing intervals are also shown by the vertical dashed lines.

Cloud droplet volume distributions for each penetration have been assembled for three different calibration schemes, described in Table 1. Scheme 1 is the calibration suggested by the manufacturer, PMS. Scheme 2 is the modified calibration suggested by Dye and Baumgardner. Scheme 3 is a modification of scheme 2 in which size bins have been combined, by the authors, in order to further reduce ambiguities associated with the response function (Fig. 1).

Five parameters have been chosen to describe the droplet distributions: the mean volume diameter (MVD), the effective diameter (D_e), the effective dispersion (V_e), the skewness (S) and the kurtosis (K). They are defined as follows:

$$\mathrm{MVD} = \left[\left(\int D^3 \cdot n \cdot dD\right) \Big/ \left(\int n \cdot dD\right)\right]^{1/3}$$

$$D_e = \left(\int D^4 \cdot n \cdot dD\right) \Big/ \left(\int D^3 \cdot n \cdot dD\right)$$

TABLE 1. Bin size limits for calibration schemes with FSSP on range 3 (see text for scheme reference).

	Scheme (μm)		
Bin	1	2	3
1	1–3	1–2.3	1–2.3
2	3–5	2.3–3.2	[2.3–
3	5–7	3.2–4.9	–4.9]
4	7–9	4.9–7.4	[4.9–
5	9–11	7.4–11.0	–
6	11–13	11.0–13.0	–13.0]
7	13–15	13.0–14.8	[13.0–
8	15–17	14.8–16.6	–
9	17–19	16.6–19.2	–19.2]
10	19–21	19.2–22.6	[19.2–
11	21–23	22.6–25.2	–25.2]
12	23–25	25.2–27.0	25.2–27.0
13	25–27	27.0–30.0	27.0–30.0
14	27–29	30.0–33.0	30.0–33.0
15	29–31	33.0–35.2	33.0–35.2

$$V_e = \left[\left(\int (D - D_e)^2 \cdot D^3 \cdot n \cdot dD\right) \Big/ \left(\int D^3 \cdot n \cdot dD\right)\right]^{1/2} \Big/ D_e$$

$$S = \left(\int (D - D_e)^3 \cdot D^3 \cdot n \cdot dD\right) \Big/ \left(\int D^3 \cdot n \cdot dD\right)$$

$$K = \left(\int (D - D_e)^4 \cdot D^3 \cdot n \cdot dD\right) \Big/ \left(\int D^3 \cdot n \cdot dD\right)$$

where D is the diameter of the droplet and $n \cdot dD$ is the number of droplets within the size interval dD. According to the above definitions, the mean volume diameter is proportional to the liquid water content (which is one of the most important measurements), the effective diameter corresponds to the mean diameter of the volume distribution, and the effective dispersion is related to the dispersion of the volume distribution. The skewness and kurtosis are variables that characterize the shape of a distribution. The skewness is a measure of the departure from symmetry of a distribution. For a normal curve, the skewness is zero.

TABLE 2. Results of the Mann-Whitney test for the intercomparison of the MVD samples. α is the significance level higher from which the null hypothesis H_0: the two samples come from the same population, is rejected.

	Data	
Scheme	Summer	Winter
	α	α
2 vs 3	0.77	0.38
1 vs 2	0.64	0.12
1 vs 3	0.77	0.34

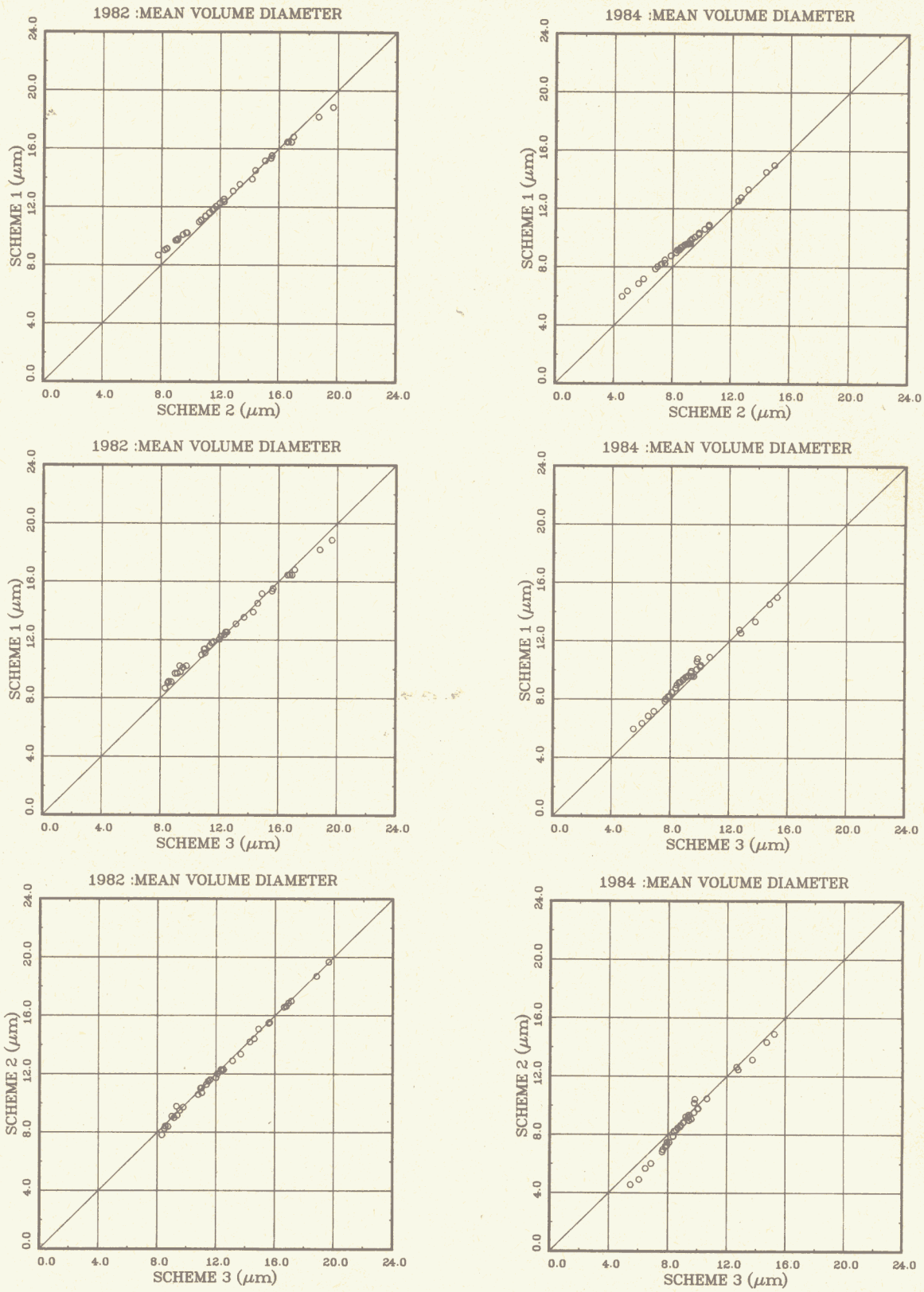

FIG. 2. Intercomparison between the MVD values calculated by the various schemes 1 vs 2, 1 vs 3 and 2 vs 3 for 1982 and 1984. If the two schemes resulted in identical MVD values, then the corresponding points will lie on the 1:1 line.

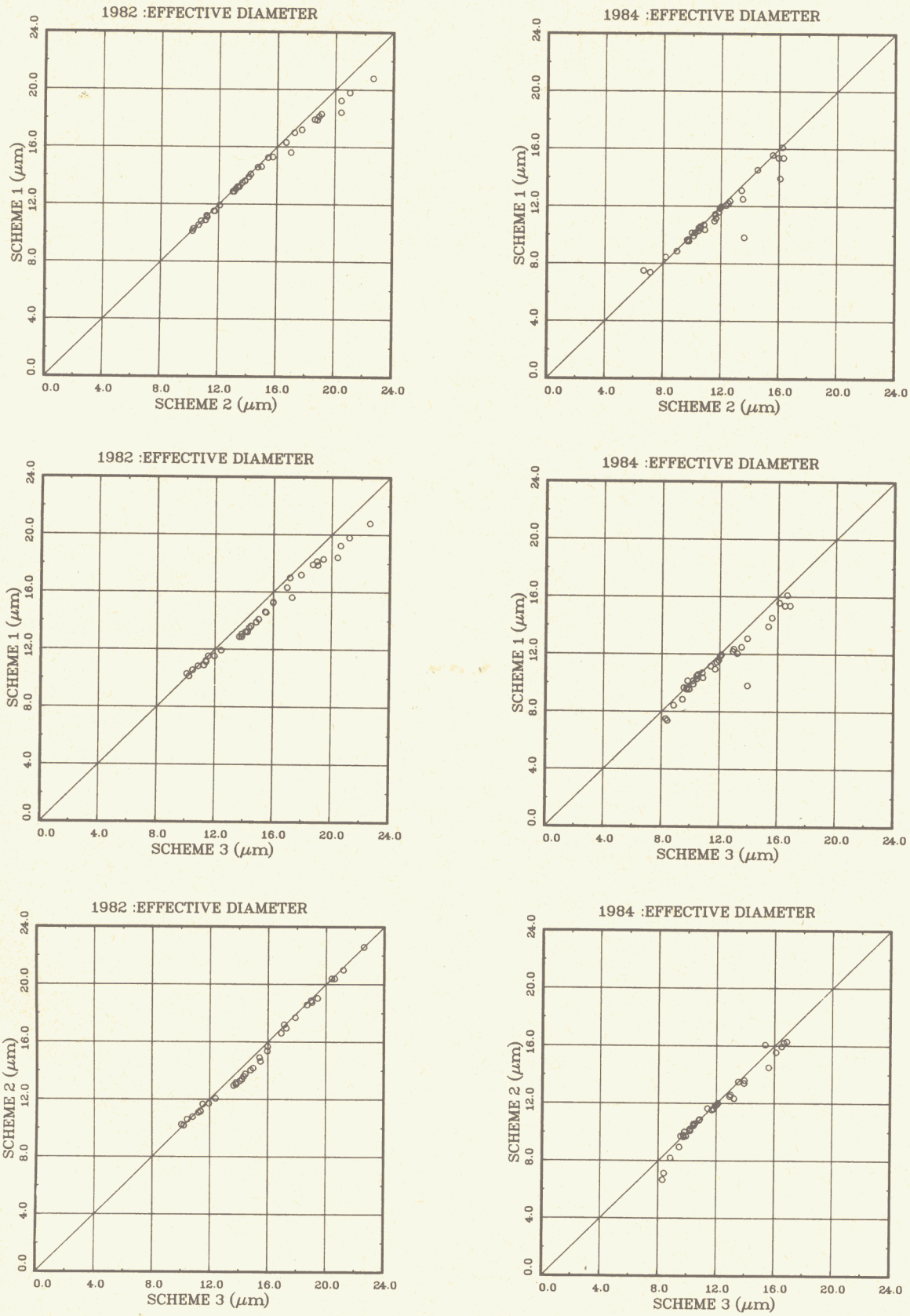

FIG. 3. As in Fig. 2 but for D_e.

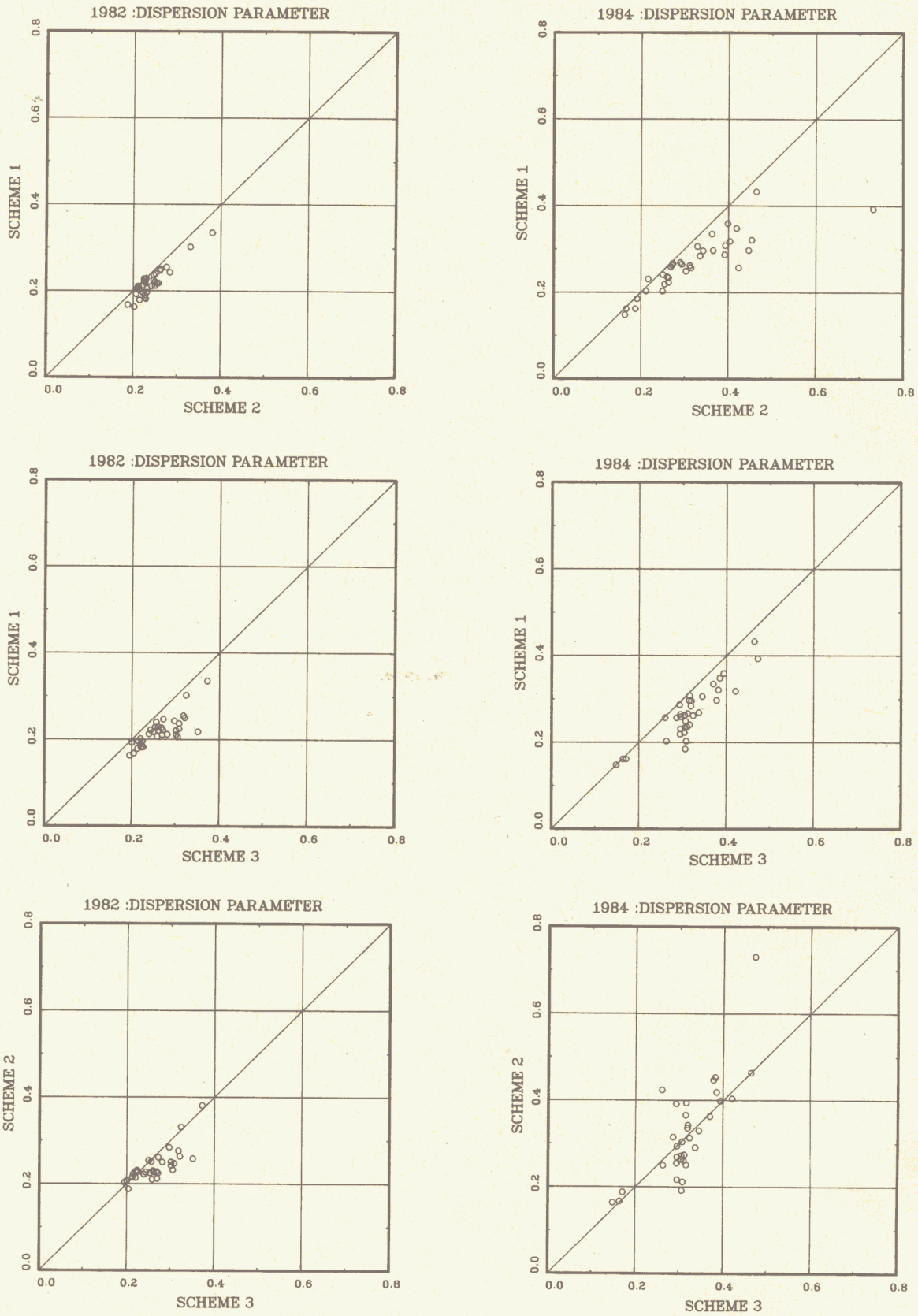

FIG. 4. As in Fig. 2 but for V_e.

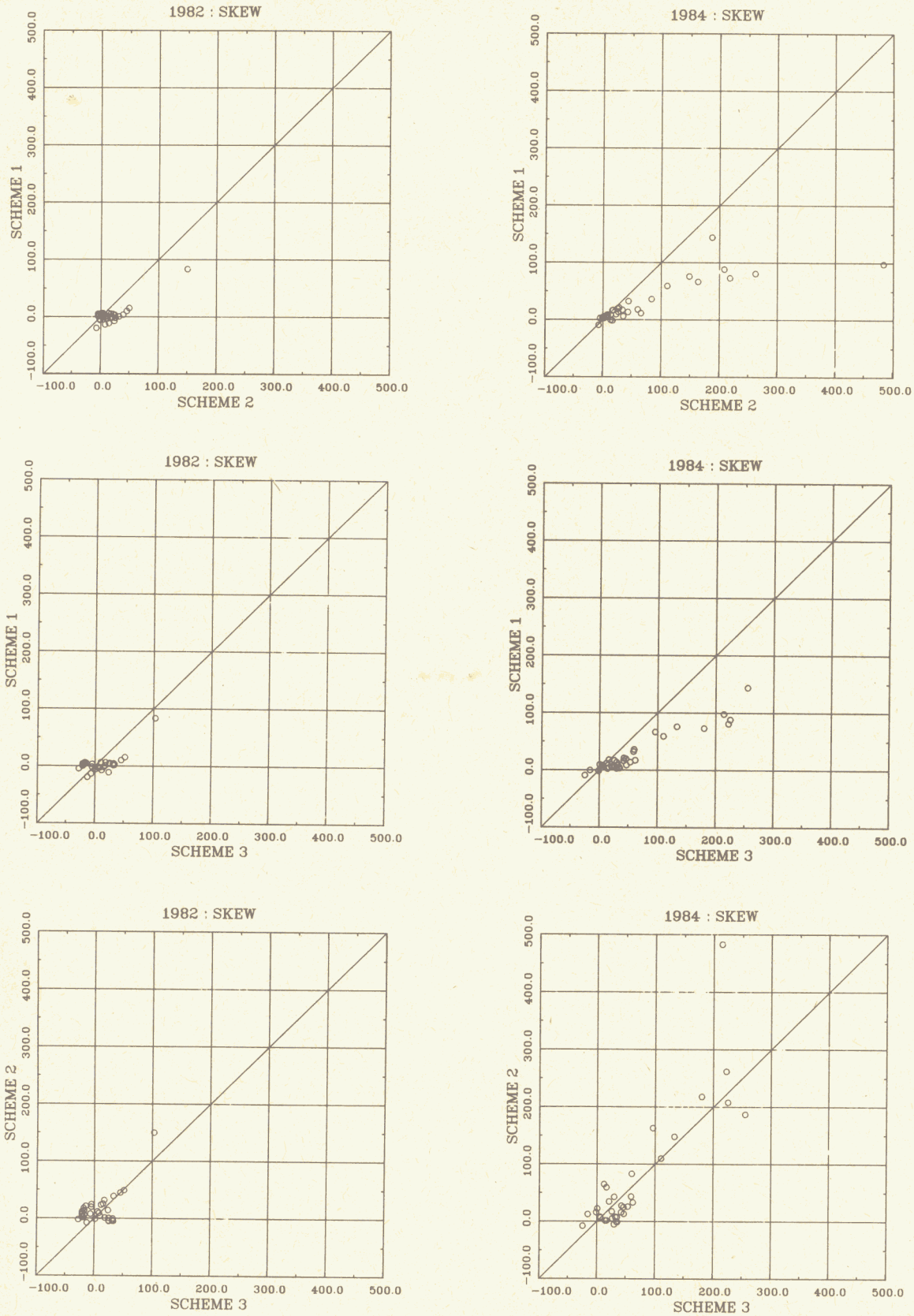

FIG. 5. As in Fig. 2 but for skewness.

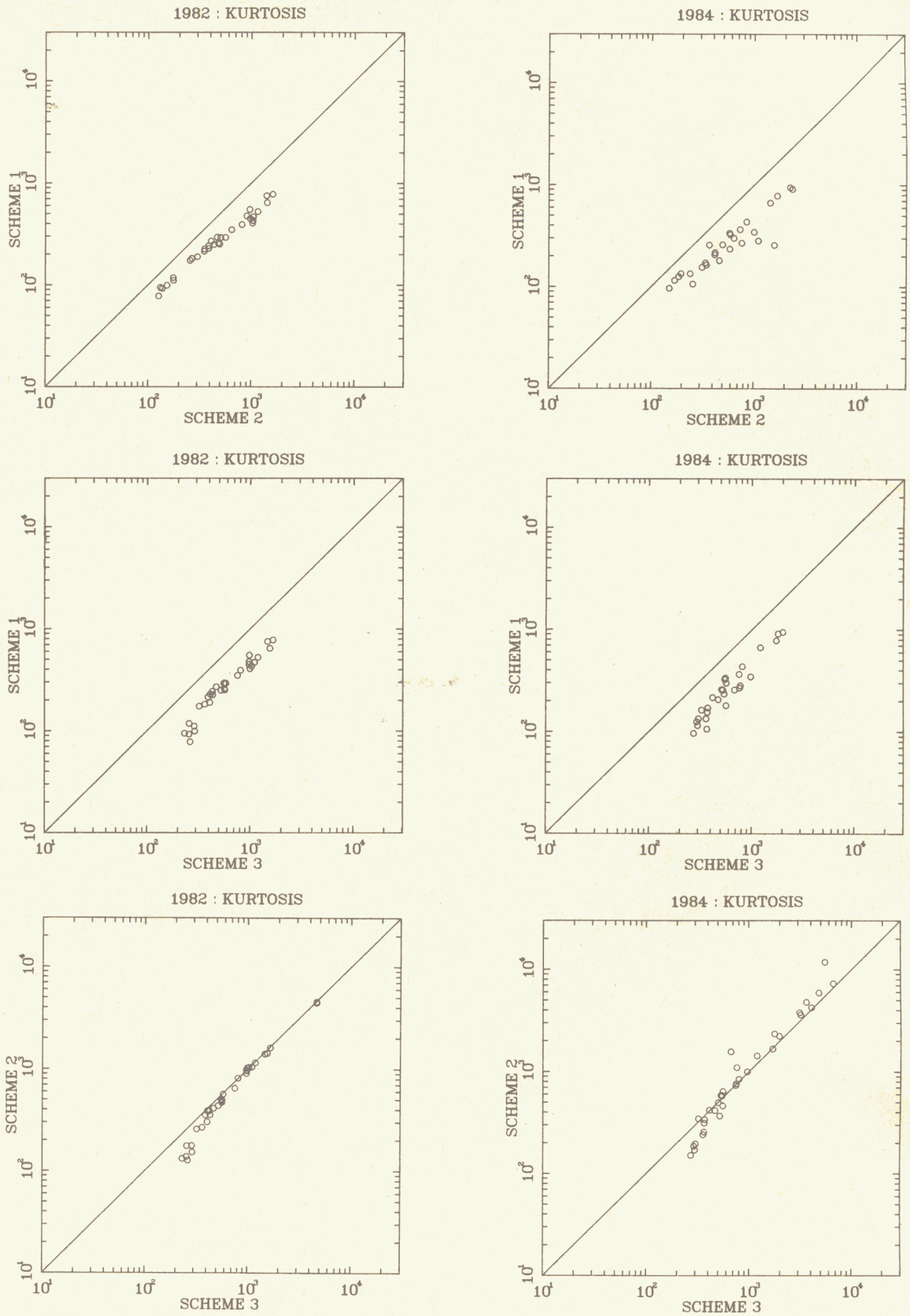

FIG. 6. As in Fig. 2 but for kurtosis.

TABLE 3. As in Table 2 but for the D_e samples.

Scheme	Data	
	Summer	Winter
	α	α
2 vs 3	0.53	0.82
1 vs 2	0.67	0.67
1 vs 3	0.36	0.45

TABLE 5. As in Table 2 but for the skewness samples.

Scheme	Data	
	Summer	Winter
	α	α
2 vs 3	0.39	0.09
1 vs 2	0.01	0.04
1 vs 3	0.04	0.00

The kurtosis measures the extent to which a distribution is peaked (leptokurtic) or flat (platykurtic).

Each scheme will result in 35 values of each parameter for each season. Therefore, for a given period and parameter we will have a group of five samples of size 35. These samples will have to be compared with each other statistically in order to determine whether or not they are significantly different.

For any two samples we are interested in testing the null hypothesis H_0: the two samples come from identical populations ($\mu_1 = \mu_2$, where μ_1 and μ_2 represent the means of the two populations). The criteria for evaluating this work is the Mann-Whitney test. This test is a distribution-free test, which means that no assumptions are made concerning the populations from which we are sampling.

According to the Mann-Whitney test, the values in the two samples are arranged jointly in an increasing order of magnitude and are assigned in this order the ranks 1, 2, 3, . . . , etc. If there is an appreciable difference between the means of the two populations, most of the lower ranks are apt to be occupied by the values of one sample while most of the higher ranks are apt to be occupied by the values of the other sample. Thus, in the Mann-Whitney test we base our decision on the ranks occupied by the values of the two samples.

3. Results and discussion

Figure 2 shows the intercomparisons between the values of MVD for summer and winter. Table 2 gives the test results of intercomparing the MVD values. The first column indicates which schemes are compared. The second and third columns give the level of significance, α, greater from which the null hypothesis, H_0, has to be rejected. If, for example, $\alpha = 0.08$, H_0 would be rejected at the significance level $\alpha = 0.1$ and would be accepted at the significance level $\alpha = 0.05$. The value of α is determined by the Mann-Whitney test. The higher the value of α the less the probability is to reject H_0. In other words, the higher the α the more similar the two samples will be. Figures 3, 4, 5 and 6 are similar to Fig. 2 but they show the intercomparison between the values of D_e, V_e, skewness and kurtosis, respectively. In turn, Tables 3, 4, 5 and 6 are similar to Table 2 but they give the test results for D_e, V_e, skewness and kurtosis, respectively.

From Table 2, it can be observed that very high values of α are reported for all summer data comparisons. This means that there are no significant differences between the three MVD samples. For the winter data, the values of α are still high (compared to typical values of α normally used in testing null hypotheses) but they are noticeably lower than those for the summer data. As can be seen in Fig. 2, scheme 2 estimates lower values for the MVD for the smaller drops when it is compared to schemes 1 and 3. These differences are more pronounced between scheme 2 and scheme 1. The corresponding α is the lowest observed and equal to 0.12 (i.e., H_0 is rejected at a significance level $\alpha > 0.12$). Because in summer the drops are usually larger, these disagreements are not as pronounced, and therefore the values of α are higher in the summer.

From Table 3 it can be observed that for both summer and winter the similarity between the D_e samples is, in general, quite strong. The degree of agreement between the D_e samples seems to be somewhat higher in the winter data (see also Fig. 3). This may suggest that the differences in D_e values (which are introduced by the different sizing schemes) are minimized when more smaller drops are present. From Fig. 3 it may also be observed that both schemes 2 and 3 estimate

TABLE 4. As in Table 2 but for the V_e samples.

Scheme	Data	
	Summer	Winter
	α	α
2 vs 3	0.03	0.62
1 vs 2	0.00	0.02
1 vs 3	0.00	0.00

TABLE 6. As in Table 2 but for the kurtosis samples.

Scheme	Data	
	Summer	Winter
	α	α
2 vs 3	0.42	0.19
1 vs 2	0.00	0.00
1 vs 3	0.00	0.00

somewhat higher D_e values for larger drops (summer data) when they are compared to scheme 1. This may be a direct result of the reduction of the ambiguities considered in both schemes. In addition, it can be observed that in the summer all schemes give almost identical results when it comes to small drops (between 8 and 12 μm). This is a reflection of the similarity of the sizing calibration schemes in this range.

From Table 4 it can be observed that the similarity between the schemes ends when it comes to V_e samples (see also Fig. 4). Except for the winter data comparison between scheme 2 and scheme 3, H_0 is rejected at $\alpha = 0.05$ for any other comparison. The very low α values suggest that the differences between the V_e samples are considerable. Similar comments can be made for the intercomparison of the skewness and kurtosis samples. As can be seen in Tables 5 and 6, except for the comparisons between scheme 2 and scheme 3, H_0 is rejected at $\alpha = 0.05$ for any other comparison (see also Figs. 5 and 6). These differences in the dispersion, the skewness and the kurtosis of the volume distributions may reflect (apart from the differences in convection between summer and winter) on the consequences of the ambiguities due to the oscillations in the scattering response (Fig. 1), the effect of which was reduced in both scheme 2 and scheme 3. This may explain the relatively higher correlation between the samples resulted from scheme 2 and scheme 3.

Some of the main conclusions of the above statistical procedure may be visualized in Fig. 7, which shows FSSP volume distributions as determined by the three different schemes. Figure 7 refers to measurements conducted in a cloud penetration on 3 February 1984. When consulting Fig. 7, the reader should note that both scales are logarithmic (which means that the differences are larger than they appear). In addition, it should be mentioned that Fig. 7 is just an individual example and may not exactly reflect the results reported in Tables 2–6, which were obtained from the considered assemblies. In Fig. 7 it is apparent that scheme 1 results in a distribution that is different in the tails than the distributions resulting from schemes 2 and 3, which appear quite similar. Scheme 1 seems to underestimate the number of the very small and very large drops and overestimate the number of the medium-size drops. As a consequence, the distribution resulted from scheme 1 appears more leptokurtic. In such a case it is possible that the dispersion, the skewness and kurtosis are affected while the mean volume diameter and effective diameter remain similar (consider, for example, a normal distribution and "press" the tails "inward" without displacement. The new distribution will have the same mean and mode, but different shape parameters).

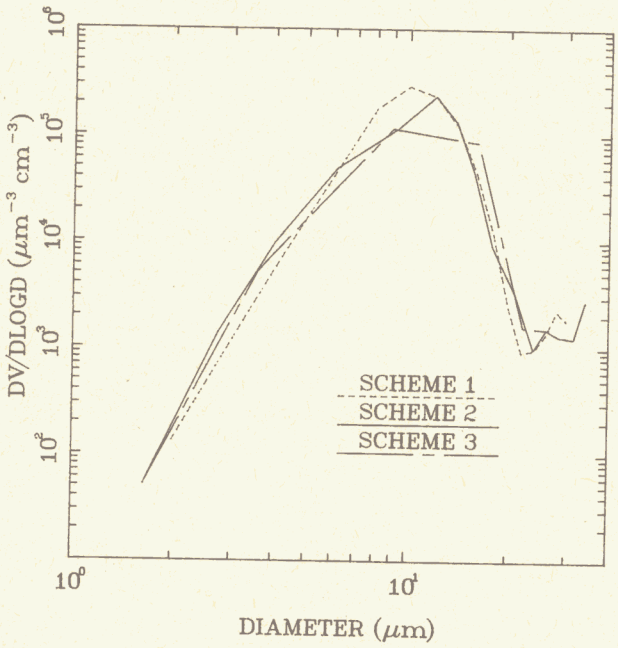

FIG. 7. FSSP volume distributions as determined by the three calibration schemes.

4. Conclusions

The choice of the calibration scheme for the FSSP from those presented has in general a small effect on the mean volume diameter (i.e., liquid water content) and effective diameter of the cloud droplet volume distribution, based upon the data from the clouds sampled in this study. This assessment is made for climatological ensembles and may not always hold for individual spectra.

The shape of the measured cloud droplet volume distribution, however, is quite sensitive to changes in the calibration. This may indicate that the oscillations in the Mie scattering response affect the shape of the droplets' volume distribution. The stronger statistical similarity, however, between the scheme 2 and scheme 3 samples may indicate that this is not the only reason. However, we hope that the reported differences in the dispersion, skewness and kurtosis results will warrant further consideration of the sizing calibration of the FSSP.

Acknowledgments. We wish to thank J. W. Strapp (of AES) for his assistance with the FSSP and M. A. Wasey (of AES) for his expert maintenance of the probe.

REFERENCES

Dye, J. E., and D. Baumgardner, 1984: Evaluation of the forward-scattering spectrometer probe. Part I: Electronic and optical studies. *J. Atmos. Oceanic Technol.*, **1**, 329–344.